JOURNAL OF CATALYSIS 132, 117–127 (1991)

Partial Oxidation of Methane to Carbon Monoxide and Hydrogen over a Ni/Al_2O_3 Catalyst

DHAMMIKE DISSANAYAKE, MICHAEL P. ROSYNEK,[1] KARL C. C. KHARAS,[2] AND JACK H. LUNSFORD

Department of Chemistry, Texas A & M University, College Station, Texas 77843

Received January 28, 1991; revised April 29, 1991

Partial oxidation of methane occurs in the temperature range 450–900°C by reaction of an oxygen-deficient CH_4/O_2 mixture over a 25 wt% Ni/Al_2O_3 catalyst. Carbon monoxide selectivities approaching 95% and virtually complete conversion of the methane feed can be achieved at temperatures >700°C. The oxidation state and phase composition of the catalyst were characterized using X-ray photoelectron spectroscopy and X-ray powder diffractometry. This study revealed that, under operating conditions, the previously calcined catalyst bed consists of three different regions. The first of these, contacting the initial $CH_4/O_2/He$ feed mixture, is $NiAl_2O_4$, which has only moderate activity for complete oxidation of methane to CO_2 and H_2O. The second region is $NiO + Al_2O_3$, over which complete oxidation of methane to CO_2 occurs, resulting in an exotherm in this section of the bed. As a result of complete consumption of O_2 in the second region, the third portion of the catalyst bed consists of a reduced Ni/Al_2O_3 phase. Formation of the CO and H_2 products, corresponding to thermodynamic equilibrium at the catalyst bed temperature, occurs in this final region, via reforming reactions of CH_4 with the CO_2 and H_2O produced during the complete oxidation reaction over the NiO/Al_2O_3 phase.

INTRODUCTION

Several important catalytic processes require either synthesis gas (H_2/CO) in various compositions or H_2 or CO separately as feedstocks. Examples include the synthesis of methanol (*1, 2*) and its carbonylation to acetic acid (*3, 4*), the Fischer–Tropsch synthesis (*5–7*), the methanol-to-gasoline process (*8, 9*), ammonia synthesis (*10*), and hydrodesulfurization (*11*). Among the most important commercial methods of synthesis gas manufacture is the steam reforming of natural gas and other light hydrocarbons (*12, 13*), which, for methane as the reactant, produces a 3 : 1 H_2 : CO product mixture:

$$CH_4 + H_2O \rightarrow CO + 3H_2. \qquad (1)$$

This process typically utilizes a dispersed nickel catalyst supported on α-Al_2O_3, MgO, or $MgAl_2O_4$ and promoted with CaO and/or K_2O (*14*). The stoichiometry and endothermicity ($\Delta H_{298} = +49.3$ kcal/mole) of Reaction (1) necessitate the use of relatively high temperatures (>800°C) and pressures (20–30 atm) to obtain acceptable yields of synthesis gas product. Because of the considerable expense associated with maintaining the reaction conditions needed for conventional steam reforming, alternative routes to synthesis gas production from methane have been examined by numerous investigators.

Among the first studies of synthesis gas formation by catalytic conversion of CH_4/O_2 mixtures was that of Prettre *et al.* (*15*), who employed a reduced 10 wt% refractory-supported nickel catalyst in the temperature range 725–900°C and 1 atm total pressure. Based on observed tempera-

[1] To whom correspondence should be addressed.

[2] Present address: Allied Signal, Inc., Des Plaines, IL.

0021-9517/91 $3.00

ture excursions in the catalyst bed under O_2-deficient conditions ($CH_4:O_2 = 2:1$), they concluded that an initial exothermic reaction was followed by an endothermic change. The exothermic behavior near the beginning of the catalyst bed was attributed to the total combustion of 25% of the CH_4 feed, which resulted in complete consumption of the stoichiometrically limited O_2 reactant,

$$CH_4 + 2O_2 \rightarrow CO_2 + 2H_2O. \quad (2)$$

The subsequent endothermic effect was ascribed to reforming of the remaining unreacted CH_4 by the H_2O and/or CO_2 produced in Reaction (2):

$$CH_4 + H_2O \rightarrow CO + 3H_2 \quad (3)$$

$$CH_4 + CO_2 \rightarrow 2CO + 2H_2. \quad (4)$$

Compositions of the final $CH_4/CO/CO_2/H_2$ reaction mixtures agreed with thermodynamic predictions under all conditions studied, indicating that thermodynamic equilibrium corresponding to the catalyst bed exit temperature was attained in all cases. Yamamoto and co-workers (*16*) proposed a similar sequence of reaction steps for the partial oxidation of C_6^+ hydrocarbons over supported nickel catalysts.

Huszár and co-workers (*17*) examined the importance of diffusion effects during methane partial oxidation by studying the reaction of 25% CH_4:air mixtures over a single grain of a series of Ni/mullite catalysts in the temperature range 760–1000°C. They concluded that the formation of H_2/CO product required the presence of reduced metallic nickel, achieved by using O_2-deficient conditions, and that the kinetics of the overall process were limited by the rate of O_2 diffusion into the catalyst pores. The effective concentration of O_2 at the catalyst surface during reaction was essentially zero, allowing the nickel to be maintained in the zero-valent state.

Gavalas and co-workers (*18*) studied the effects of calcination temperature, prereduction, and feed ratio on the catalytic behavior of NiO/α-Al_2O_3 for conversion of CH_4/O_2 mixtures at 570–760°C. For CH_4/O_2 feed ratios of 1.3 to 1.7, they observed a decrease in initial activity with increasing calcination temperature, which they attributed to changes in the surface Ni^{3+} concentration, and a decline in activity with increasing time-on-stream. The principal reaction products in all cases under these conditions were CO_2 and H_2O. Prereduction in H_2 at 650–760°C caused the initial activity to increase by one to three orders of magnitude, depending upon prior calcination temperature. The authors believed that the zero-valent nickel produced by prereduction reverted to NiO under the reaction conditions employed, resulting again in a decline in activity with increasing time-on-stream. At a reaction temperature of 710°C, CO_2 remained the only carbon-containing product until the CH_4/O_2 feed ratio was increased to >8, at which point CO and CO_2 were produced in comparable amounts.

Very recently, Green and co-workers studied the partial oxidation of CH_4 over mixed metal oxides of ruthenium (*19*) and over a range of supported transition metals (*20*). They reported that CH_4/O_2 feed ratios ≥ 1.7 could be converted in a very high yield (>90%) to H_2/CO product at reaction temperatures $\gtrsim 750$°C. Calculations indicated that virtual thermodynamic equilibrium was achieved under these reaction conditions. Increasing the total pressure and decreasing the reaction temperature caused decreases in both CH_4 conversion and CO/CO_2 product ratio, in agreement with thermodynamic equilibrium predictions. The authors postulated that the reaction pathway in all cases may involve initial conversion of a fraction of the CH_4 feed to CO_2 and H_2O, followed by the occurrence of steam reforming and reverse water–gas shift reactions.

In view of increased recent interest in methane-selective oxidation processes, the present study was undertaken to examine in greater detail the behavior of a supported nickel catalyst for the conversion of CH_4/O_2 feeds to H_2/CO product mixtures under O_2-

deficient conditions. Particular emphasis was placed on characterizing the chemical composition of the catalyst under reaction conditions and the changes in nickel oxidation state caused by variations in reaction temperature, CH_4/O_2 feed ratio, and contact time. The reaction results have been compared to CH_4 conversions and CO/CO_2 product ratios predicted by thermodynamic equilibrium calculations.

EXPERIMENTAL

Materials

The nickel catalyst employed in this study was a commercial material (C11-2S-06) manufactured by United Catalysts Co. for the steam reforming of light hydrocarbons. This catalyst has also been previously studied for CO_2 reforming of methane (*21*). The catalyst had a Ni loading of 25 wt% (reduced basis) and a total BET–N_2 surface area of 22 m^2/g. The support consisted of Al_2O_3: TiO_2: CaO in the molar ratio 7 : 2 : 1. X-ray powder diffraction analysis by Gadalla and Sommer indicated that the unreduced catalyst contained α- and γ-Al_2O_3, NiO, $CaO \cdot 2Al_2O_3$, and $CaO \cdot 3TiO_2 \cdot 4Al_2O_3$ (*21*). The original catalyst cylinders were crushed and sieved to 20- to 40-mesh granules before use. Methane (99.99%) from Matheson and helium (99.995%) and oxygen (99.9%) from Airco were used without further purification.

Procedures

All experiments were performed using a tubular quartz reactor having an internal diameter of 0.25 cm and an axial thermowell containing a chromel–alumel thermocouple centered in the catalyst bed and used for temperature measurement and control. A 50-mg catalyst sample was used for all runs, except those requiring very high space velocities, for which a 25- or 12.5-mg sample was employed. The catalyst bed was 1.5 cm long for a 50-mg sample and was preceded by a 1.5-cm preheating region containing 20- to 45-mesh quartz chips (Fig. 1). Control experiments using an empty reactor and one

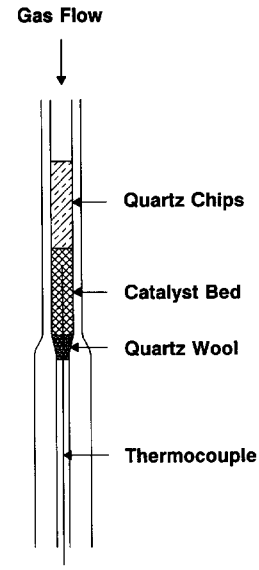

FIG. 1. Schematic representation of the flow reactor.

containing only quartz chips demonstrated that conversion of CH_4 at 800°C was <1% in the absence of a catalyst. The catalyst was pretreated in a 1 : 1 mixture of either O_2 : He or H_2 : He for 6 h at 600°C, using a total flow rate of 50 cm^3/min. X-ray diffractometry and X-ray photoelectron spectroscopy (see below) confirmed that the nickel was completely reduced to the zero-valent state by the H_2 treatment, and to a mixture of nickel oxide (NiO) and nickel aluminate ($NiAl_2O_4$) by the O_2 treatment. Reactions were typically performed using a feed mixture of $CH_4 : O_2 : He = 1.78 : 1 : 25$ at a total flow rate of 50 cm^3/min and a total pressure of 1 atm, resulting in an effective contact time of ~0.09 s. Space velocity was varied, when desired, by changing the flow rate of He, while maintaining the CH_4 and O_2 flows constant.

Analyses of reactant/product mixtures were made by periodically directing the reactor effluent through the sample loop of a gas sampling valve in a Varian Model 3700 gas chromatograph, which contained two columns in a series/parallel arrangement. Separation of CO_2 and H_2O from the re-

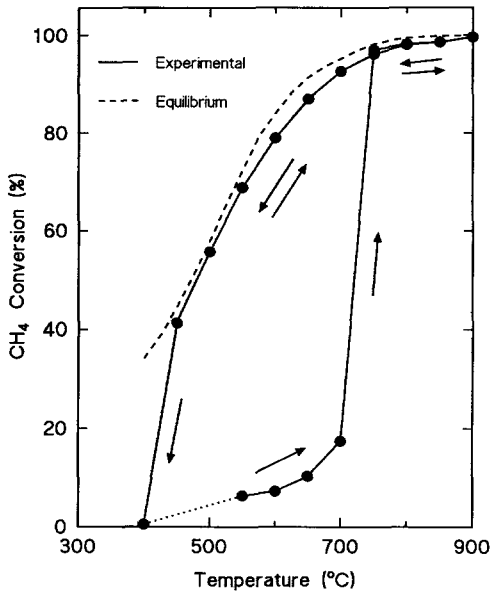

FIG. 2. Effect of reaction temperature on conversion of CH_4 over precalcined Ni/Al_2O_3 (CH_4/O_2 = 1.78; S.V. = 750 vol/vol/h).

maining components occurred on a 6 ft × ⅛ in. o.d. stainless steel column containing 80- to 100-mesh Chromosorb 107 at 150°C, while separation of H_2, O_2, CH_4, and CO was accomplished on a 6 ft × ⅛ in. o.d. stainless steel column containing 60- to 70-mesh 13X molecular sieve at 0°C. Prior to passage through the thermal conductivity detector, the effluent from the latter column was passed through a 1 ft × ¼ in. o.d. stainless steel column containing CuO at 500°C in order to convert eluted H_2 to H_2O, which allowed quantitative determination of the H_2 component.

X-ray photoelectron spectroscopy (XPS) studies were performed using a Hewlett–Packard Model 5950A ESCA spectrometer, equipped with a Surface Science Laboratories Model 9261 ESCA Interface to permit computer-controlled instrument operation and data acquisition and analysis. Monochromatic Al$K\alpha$ radiation (1486.6 eV) was used as the excitation source in all cases, and an electron flood gun was used to provide charge neutralization of the non-conducting samples. The C 1*s* peak at 284.6 eV due to adventitious carbon was used as an internal standard. The sample probe of the instrument was contained within a controlled atmosphere glove box to permit the introduction of previously treated samples into the instrument's analyzer chamber without exposure to atmospheric O_2 and H_2O. In order to obtain spectra of used catalyst samples, the CH_4 and O_2 reactant flows were stopped simultaneously with the catalyst at the desired temperature, and the reactor was then flushed and cooled in He before being sealed and transferred to the glove box of the XPS instrument.

X-ray powder diffraction (XRPD) data were obtained on a Rigaku RU-200 automated powder diffractometer, using Cu$K\alpha$ radiation generated at 50 kV and 180 mA. Data were collected by step scan methods within a 2θ region of 20–75°, which encompassed the major peak(s) of the compounds being investigated.

Quantitative determinations of surface carbon contents were made by stopping the

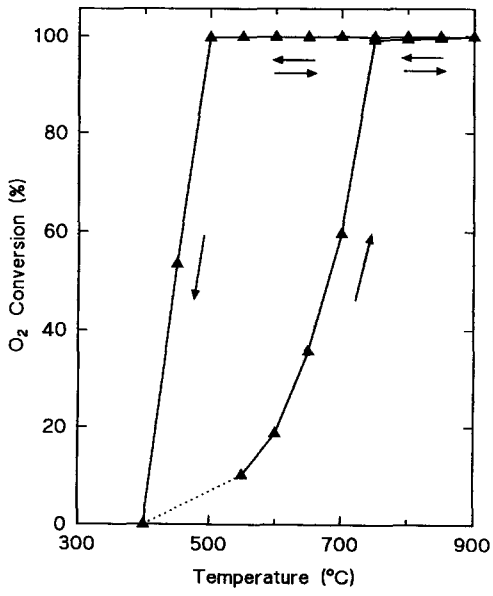

FIG. 3. Effect of reaction temperature on conversion of O_2 over precalcined Ni/Al_2O_3 (CH_4/O_2 = 1.78; S.V. = 750 vol/vol/h).

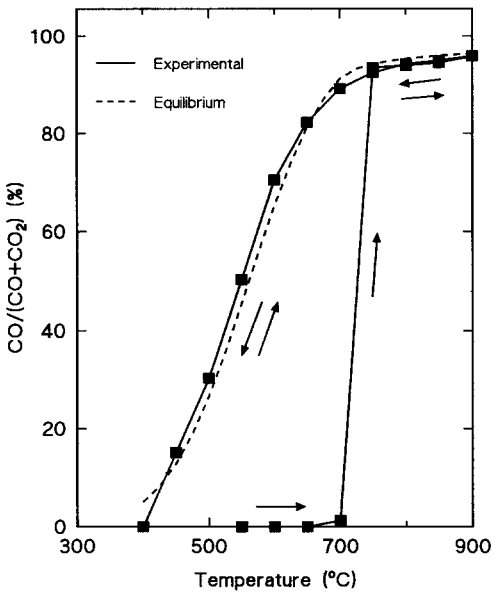

FIG. 4. Effect of reaction temperature on CO selectivity during conversion of CH_4 over precalcined Ni/Al_2O_3 (CH_4/O_2 = 1.78; S.V. = 750 vol/vol/h).

CH_4 flow during an experiment, while continuing to flow O_2 and He over the catalyst at 800°C. Chromatographic measurement of the CO_x evolved during O_2 treatment yielded the carbon content of the used catalyst.

RESULTS

Effect of Temperature on Reaction Behavior

The effect of a cycle of sequential changes in reaction temperature on the conversions of CH_4 and O_2 and on the reaction selectivity to CO is depicted for a typical experiment with a precalcined catalyst sample in Figs. 2–4. After each change in reaction temperature, the system was allowed to reattain a steady-state condition (typically requiring ~30 min) before the reaction mixture was sampled for analysis. In several instances when longer reequilibration times were allowed (viz., 60–120 min), no differences were observed in either catalytic activity/selectivity or bulk/surface compositions from those obtained after a 30 min period. At the initial reaction temperature of 550°C, conversion of CH_4 was only 6%, and the sole reaction products were CO_2 and H_2O. As the temperature was increased stepwise to 700°C, the conversion of CH_4 increased to 16%, but total oxidation to CO_2 and H_2O remained the dominant reaction.

A further increase in reaction temperature to 750°C, however, resulted in a sudden change in both activity and selectivity. Conversions of both CH_4 and O_2 increased to virtually 100%, and 95% of the 1 : 2 mixture of $CO_2 : H_2O$ total oxidation products observed at the lower temperatures was replaced by a 1 : 2 mixture of $CO : H_2O$. Further stepwise increases in reaction temperature to 900°C caused little additional change in either activity or selectivity. Most of the catalyst bed, which had been light blue-green at reaction temperatures ≤700°C, became black at ≥750°C, with only the uppermost portion of the catalyst (less than 10%) remaining blue-green at the higher temperatures. The temperature in the narrow (~1–2 mm) transition zone between the upper light blue-green region and the lower black region was ~50°C higher than that of the remainder of the catalyst bed, indicative of a highly exothermic process occurring in this zone. At a constant reaction temperature of 800°C, increases in the total reactant flow rate or decreases in the $CH_4 : O_2$ reactant ratio caused the narrow transition zone and, hence, the exothermic reaction, to move further down the catalyst bed, at the expense of the lower black region, as observed by Phichitkul (*22*). At sufficiently high flow rate or low $CH_4 : O_2$ ratio, conversion of O_2 became incomplete, causing the entire catalyst bed to revert to its original light blue-green color, and total oxidation to CO_2 and H_2O again became the predominant reaction.

When the reaction temperature of the original 1.78 : 1 mixture of $CH_4 : O_2$ was subsequently decreased at 50° intervals from 900 to 400°C, the conversions of both CH_4 and O_2 and the selectivity to CO did not retrace the pathways observed during the initial temperature increase. Conversion of

O_2 remained 100% at all reaction temperatures ≥500°C, while CH_4 conversion, by contrast, decreased gradually with decreasing reaction temperature, remaining >40% at 450°C. At 400°C, conversions of both reactants decreased to zero. Selectivity to CO also decreased gradually but continuously with decreasing temperature, while maintaining a H_2/CO product ratio of 2/1, until all reaction ceased at ~400°C. Provided that the reaction temperature was not decreased below ~450°C, conversions of both CH_4 and O_2 and the selectivity to CO continued to be described by the upper curves in Figs. 2–4, i.e., those attained after the initial sudden increase in conversion and selectivity at 750°C, throughout repeated increases and decreases in reaction temperature in the range 450–900°C. After the temperature had been decreased to 400°C, however, subsequent increases in reaction temperature resulted in the same behavior as that observed originally with the freshly calcined catalyst.

When the same cycle of experiments was repeated using a catalyst sample that had been pretreated in flowing H_2 at 600°C following calcination, the CH_4 and O_2 conversions and CO selectivity were immediately described by the upper curves in Figs. 2–4, without undergoing the initial low-temperature behavior exhibited by the calcined, but unreduced, catalyst. At all reaction temperatures ≥450°C, the reaction behavior again followed these upper curves during repeated sequences of temperature increases and decreases.

Surface Carbon Deposition

Under the low-temperature (≤700°C) reaction conditions over the calcined catalyst, which produced only CO_2 and H_2O products, deposition of surface carbon did not occur, as shown by the absence of evolved CO_x when the CH_4 flow was stopped. Following the sudden increases in CH_4 and O_2 conversions that occurred at ~750°C, the total surface carbon content of the catalyst had increased to ~1 monolayer. This behavior is depicted in Fig. 5, which displays XPS

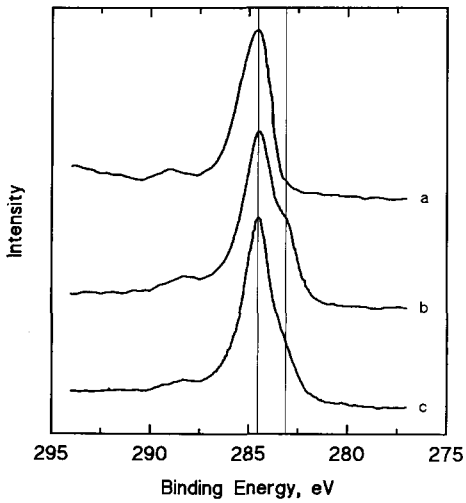

FIG. 5. XPS spectra of Ni/Al_2O_3 in C 1*s* region for (a) freshly calcined sample; (b) following CH_4/O_2 reaction at 800°C, and (c) following subsequent CH_4/O_2 reaction at 500°C.

spectra in the C 1*s* region for a freshly calcined sample and for one that had been used under reaction conditions at 800°C. The prominent peak at a binding energy of 284.6 eV in each spectrum is due to adventitious carbon, while the small peak at ~288 eV, which remained virtually unchanged throughout the cycle of reaction temperatures investigated, may be due to residual surface CO_3^{2-}. Spectrum b reveals the appearance of a new C 1*s* peak at ~283.3 eV, attributed to a graphitic or carbidic surface carbon species that was deposited during reaction at 800°C. The intensity of this added peak decreased markedly following subsequent reaction at 500°C (spectrum c).

At reaction temperatures ≥750°C, the amount of surface carbon generated was primarily influenced by the $CH_4 : O_2$ feed ratio. At $CH_4 : O_2$ ratios ≥2, the reaction produced large amounts of surface carbon that filled the catalyst pores and caused the granules to disintegrate into a fine powder. When the $CH_4 : O_2$ ratio was ≤1.25, the catalyst reverted to its low-activity state, which produced only CO_2 and H_2O products, but no significant surface carbon. At the $CH_4 : O_2$

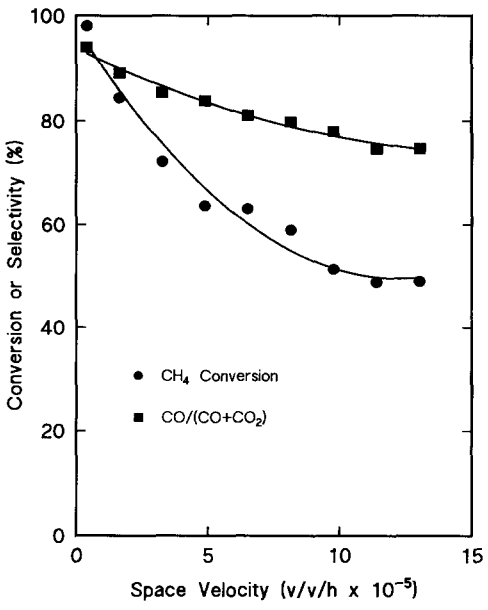

FIG. 6. Effect of space velocity on CH_4 conversion and CO selectivity (CH_4/O_2 = 1.78).

ratio of 1.78 employed for the experiment depicted in Figs. 2–4, the steady-state concentration of surface carbon (~1 monolayer) caused no observable decrease in catalytic activity, even after 50 h of continuous reaction at 800°C.

Reaction Thermodynamics

Reaction mixture compositions observed for the upper curves in Figs. 2–4 agreed closely with those corresponding to thermodynamic equilibrium at each temperature, as shown by the dashed curves included in each of these figures. The thermodynamic data shown were calculated for the $CH_4 : O_2$ reactant ratio of 1.78 : 1 using a free energy minimization technique, and represent the components CH_4, CO, CO_2, H_2O, H_2, and O_2 (*23*). For the $CH_4 : O_2$ reactant ratio used in these experiments, the equilibrium conversion of O_2 was 100% throughout the range of reaction temperatures investigated. (More than 90 additional components in the C–H–O system were included in the free energy calculations, but all had equilibrium mole fractions of $< 1 \times 10^{-6}$.) Deviations from thermodynamic equilibrium occurred when the contract time was sufficiently decreased by increasing the total reactant flow rate. This behavior is shown in Fig. 6 for a reaction temperature of 800°C

Catalyst Characterization

The markedly different *initial* behaviors of the unreduced and reduced catalysts indicated that a decrease in nickel oxidation state may be responsible for the sudden changes in activity and selectivity that were observed for a calcined, unreduced catalyst at a reduction temperature of ~750°C. In order to more fully characterize the oxidized and reduced Ni phases that caused the observed differences in catalytic behaviors, XRPD patterns and XPS spectra were obtained for catalyst samples following operation at various reaction temperatures over the entire temperature cycle investigated. Bulk phases identified by XRPD in the freshly calcined, unreduced catalyst were α-Al_2O_3, TiO_2 (rutile), $CaTiO_3$, NiO, and the

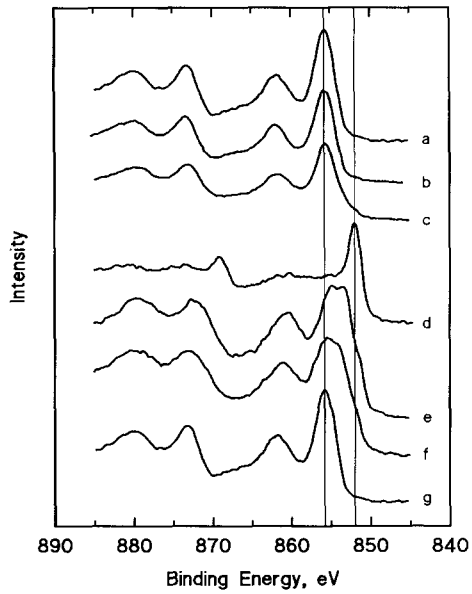

FIG. 7. XPS spectra of Ni/Al_2O_3 in Ni 2*p* region for (a) freshly calcined sample; and following sequential CH_4/O_2 reaction at (b) 550°C; (c) 725°C; (d) 800°C; (e) 550°C; (f) 500°C; and (g) 300°C.

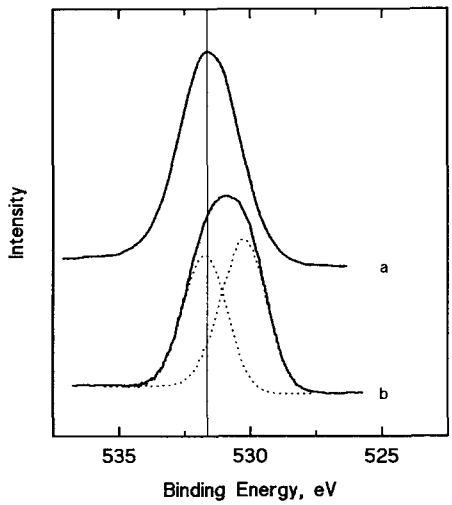

FIG. 8. XPS spectra of Ni/Al_2O_3 in O 1*s* region, (a) following CH_4/O_2 reaction at 800°C, and (b) following subsequent CH_4/O_2 reaction at 500°C.

light blue-green spinel $NiAl_2O_4$, the latter two in an approximately 60:40 ratio. No Ti–Ni–O or Ca–Ni–O phases were observed by XRPD in any of the samples examined in this study.

Figure 7 presents XPS spectra in the Ni 2*p* region for a series of experiments that each employed a sample of the calcined, unreduced catalyst as a starting material. Because of the small amount of catalyst used in these experiments, the entire used catalyst bed was required in each case to prepare a wafer of sufficient size for XPS analysis. Hence, differing regions, if any, of the catalyst bed were not separately analyzed. Following exposure to the $CH_4:O_2$ reaction mixture at any temperature below that at which the CH_4 conversion and CO selectivity suddenly increased (spectra a, b, and c), the environment of Ni, as probed by XPS, in the near-surface region (i.e., the uppermost 10–15 Å) of the sample was characteristic only of $NiAl_2O_4$, as shown by the Ni $2p_{3/2}$ peak at a binding energy of ~856 eV, with an accompanying shake-up satellite peak at ~862 eV (*24, 25*). However, after operation at a reaction temperature of 800°C, the spectrum was that of zero-valent Ni metal, characterized by a narrowed Ni $2p_{3/2}$ peak at a binding energy of ~852 eV and the absence of a significant satellite peak (*25, 26*). The O 1*s* spectrum of this sample (Fig. 8a) contained only a single peak at 531.6 eV, characteristic of pure Al_2O_3. The XRPD pattern observed for the sample used at 800°C was consistent with the XPS spectra for this material; the only identifiable phases were α-Al_2O_3, TiO_2 (rutile), $CaTiO_3$, and metallic Ni.

When the reaction temperature was decreased in stages from 800 to 300°C, the catalyst exhibited transitions among three different phases during a gradual but complete reoxidation of the near-surface region of the sample to the original $NiAl_2O_4$, which was the only phase observed at sufficiently low temperature. Metallic Ni was present in decreasing amounts at both 550 and 500°C, while NiO, characterized by the closely spaced doublet due to the presence of both Ni^{2+} and Ni^{3+} (*26–28*), was also observed following reaction at both of these temperatures. The substitution of Ni/NiO into the near-surface region of the α-Al_2O_3 structure, which produces a surface Ni environment characteristic of $NiAl_2O_4$, extends only slowly into the subsurface region of the sample at these temperatures. The XRPD pattern of the catalyst used at 550°C, for example, revealed that Ni in the bulk of the sample was primarily in the form of reduced metallic Ni, with only traces of $NiAl_2O_4$ and NiO being detected. Following use at 400°C, however, the form of Ni in the bulk sample was principally $NiAl_2O_4$ and NiO. The O 1*s* spectrum of the sample used at 500°C (Fig. 8b) exhibited a broad peak centered at ~531 eV, which contained the unresolved O 1*s* peaks of Al_2O_3 and $NiO/NiAl_2O_4$. Of particular interest was the composition of the blue-green/black transition zone that corresponded to the occurrence of the exothermic reaction described above. Following reaction at 750°C over a larger (100 mg) catalyst sample, the catalyst bed was carefully removed from the reactor in layers, in order to preserve the location of the transition

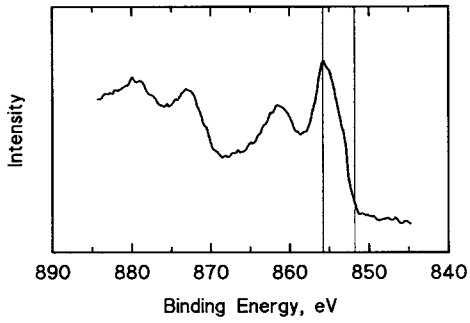

FIG. 9. XPS spectrum in Ni 2*p* region of "transition zone" of Ni/Al_2O_3 following CH_4/O_2 reaction at 750°C.

zone. The resulting XPS spectrum (Fig. 9) revealed that metallic Ni was absent from the near-surface region of the sample in the upper portion of the catalyst bed, which consisted primarily of a mixture of NiO and $NiAl_2O_4$.

DISCUSSION

The XPS and XRPD data presented in the previous section clearly demonstrate that the sudden change in behavior of the catalyst that occurs at ~750°C in Figs. 2–4 and is manifested as marked increases in the conversions of CH_4 and O_2 and in selectivity to CO and H_2 products is due to reduction of surface nickel to the metallic state. Figure 10 schematically illustrates the sequence of catalyst bed surface compositions that exist at selected temperatures along the reaction cycle depicted in Figs. 2–4. Following precalcination at 600°C, the nickel in the near-surface region of the catalyst at the initial reaction temperature of 550°C in Fig. 2 is primarily in the form of a $NiAl_2O$ phase. This material exhibits a moderate activity at this temperature (~6% conversion of CH_4 under the conditions employed) for the total oxidation of methane to CO_2 and H_2O, which gradually increases with increasing temperature to ~16% conversion at 700°C. As the temperature is further increased, however, the decrease in O_2 concentration caused by the CH_4 oxidation reaction eventually allows a portion of the $NiAl_2O_4$ near the reactor inlet to undergo thermal decomposition during a narrow interval within the temperature range 700–750°C, regenerating α-Al_2O_3 plus a surface NiO phase that has an activity much higher than that of $NiAl_2O_4$ for methane conversion to CO_2 and H_2O. Consequently, complete consumption of all the remaining O_2 and 25% of the CH_4 from the O_2-deficient CH_4/O_2 feed mixture occurs over the NiO in the highly exothermic total oxidation process, resulting in an ~50°C temperature increase in this narrow zone of the catalyst bed. The resulting $CH_4/CO_2/H_2O$ mixture quickly reduces the nickel in the rest of the catalyst bed to Ni^0, which then catalyzes reforming reactions of the remaining 75% of the CH_4 with the CO_2 and H_2O, resulting in the observed 1 : 2 CO/H_2 product mixture. The catalyst employed in this study has been previously reported, for example, to be effective for the CH_4/CO_2 reforming reaction (*21*). The overall sequence of reactions may be represented by Reactions 2–4 proposed previously by Prettre and co-workers (*15*).

Following initial attainment of reduced

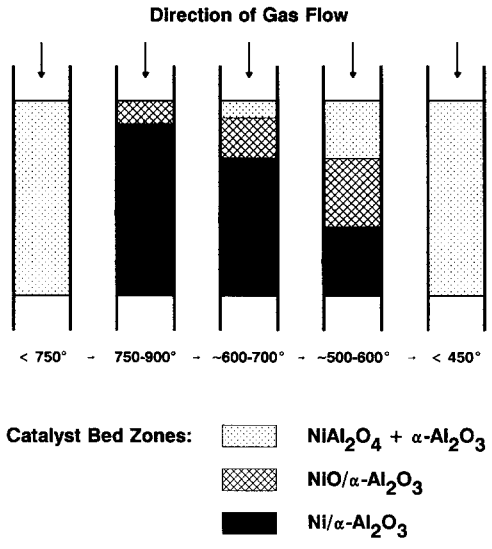

FIG. 10. Schematic representation of Ni/Al_2O_3 catalyst bed composition during CH_4/O_2 reaction at various temperatures.

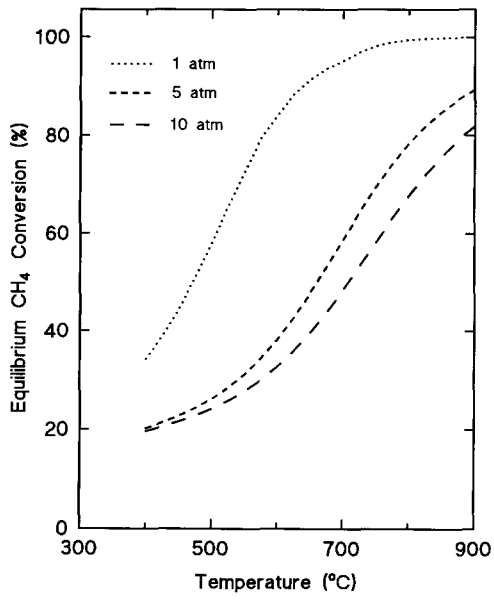

FIG. 11. Effect of temperature and pressure on equilibrium conversion of initial CH_4/O_2 = 1.78 reaction mixture.

Ni^0 at ~750°C, the composition of the reaction mixture thereafter conforms to thermodynamic equilibrium corresponding to the catalyst bed temperature throughout repeated cycles of reaction temperature within the range 450–900°C. Green and coworkers have previously reported observing virtually equilibrium conversions of 2:1 $CH_4:O_2$ mixtures at 777°C and 1 atm over a series of mixed ruthenium oxides (*19*). Sufficiently large decreases in contact time cause deviations from equilibrium (Fig. 5), due to incomplete reaction of CH_4 with CO_2 and H_2O, but conversion of O_2 remains 100% at all temperatures ≥450°C. Within this temperature range, decreases in reaction temperature result in reoxidation of a portion of the Ni^0, causing the exothermic NiO zone to broaden and move downward along the catalyst bed. This change in catalyst bed composition is completely reversible within the above temperature limits. However, if the reaction temperature is decreased below ~450°C, or if the contact time is sufficiently decreased, breakthrough of unreacted O_2 occurs, causing all of the reduced nickel on the surface to reoxidize to a $NiAl_2O_4$ phase. All reaction then ceases, since the activity of the latter for total oxidation of methane is too low to be observed at ≤400°C. Following such complete reoxidation of nickel, reattainment of thermodynamic equilibrium can be achieved only by again increasing the reaction temperature to ≥~750°C to regenerate reduced Ni^0, or by prereducing the calcined catalyst in H_2.

Separate experiments designed to elucidate the mechanism of synthesis gas formation from methane were not performed during the present investigation. However, it appears likely that surface carbon deposited during the reaction plays an important role in CO_x formation. XPS spectra such as those in Fig. 5 revealed that a constant amount of surface carbon, which decreased with decreasing reaction temperature, was maintained at each temperature in the range 450–900°C. Temporary stoppage of the CH_4 flow during an experiment resulted in reaction of the previously deposited surface car-

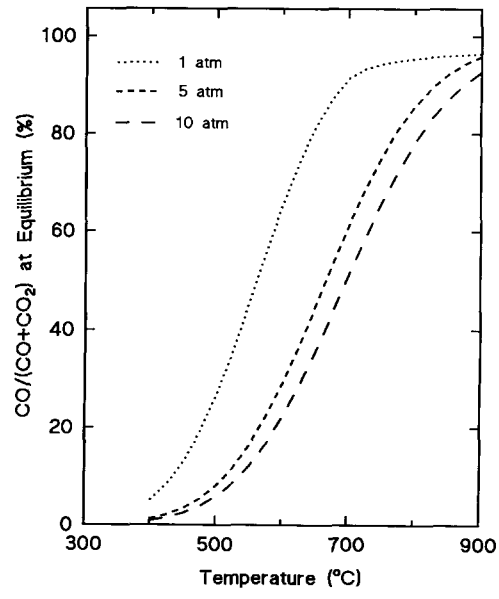

FIG. 12. Effect of temperature and pressure on equilibrium CO selectivity for conversion of initial CH_4/O_2 = 1.78 reaction mixture.

bon with the continuing O_2 feed, producing a CO/CO_2 mixture whose composition conformed to the thermodynamic equilibrium ratio at the reaction temperature employed (Fig. 4). Similarly, exposure of a precalcined catalyst sample to pure CH_4 at 800°C generated CO_2, H_2O, and surface carbon, indicating that CH_4 can effect partial reduction of $NiO/NiAl_2O_4$ to surface Ni^0 at this temperature. Exposure of a prereduced catalyst sample to CH_4 at the same temperature, however, resulted in the formation of CO, H_2, and surface carbon.

Although all experiments in the present study were performed using a total pressure of 1 atm, extension of the thermodynamic calculations to higher pressures indicates that equilibrium CH_4 conversions of >80% with CO selectivities >90% could be attained at 900°C at total reaction pressures as high as 10 atm, as shown in Figs. 11 and 12. Thus, the production of synthesis gas from CH_4/O_2 mixtures may be feasible at the super-atmospheric pressures preferred for commercial operation.

ACKNOWLEDGMENT

The authors gratefully acknowledge financial support of this research by the National Science Foundation under Grant CHE-9005808.

REFERENCES

1. Marschner, F., and Moeller, F. W., *in* "Applied Industrial Catalysis" (B. E. Leach, Ed.), Vol 2, Academic Press, New York, 1983.
2. Kung, H. H., *Catal. Rev. Sci. Eng.* **22,** 235 (1981).
3. Roth, J. F., *Platinum Metal Rev.* **19,** 12 (1975).
4. Eby, R. T., and Singleton, T. C., *in* "Applied Industrial Catalysis" (B. E. Leach, Ed.), Vol. 1, Academic Press, New York, 1983.
5. Dry, M. E., *in* "Catalysis: Science and Technology" (J. R. Anderson and M. Boudart Eds.), Vol. 1, Springer Verlag, New York, 1981.
6. Dry, M. E., *in* "Applied Industrial Catalysis" (B. E. Leach, Ed.), Vol. 2, Academic Press, New York, 1983.
7. Anderson, R. B., "The Fischer–Tropsch Synthesis," Academic Press, New York, 1984.
8. Chang, C. D., *in* "Methane Conversion" (D. M. Bibby *et al.*, Eds.), Elsevier, New York, 1988.
9. Chang, C. D., *Catal. Rev. Sci. Eng.* **25,** 1 (1983).
10. Emmett, P. H., *in* "The Physical Basis for Heterogeneous Catalysis" (E. Drauglis and R. I. Jaffee, Eds.), Plenum, New York, 1975.
11. Schuit, G. C. A., and Gates, B. C., *Am. Inst. Chem. Eng. J.* **19,** 417 (1973).
12. Trimm, D. L., *Catal. Rev. Sci. Eng.* **16,** 155 (1977).
13. van Hook, J. P., *Catal. Rev. Sci. Eng.* **21,** 1 (1981).
14. Rostrup-Nielsen, J. R., *in* "Catalysis: Science and Technology" (J. R. Anderson and M. Boudart, Eds.), Vol. 5, Springer Verlag, New York, 1984.
15. Prettre, M., Eichner, C., and Perrin, M., *Trans. Faraday Soc.* **43,** 335 (1946).
16. Yoshitomi, S., Morita, Y., and Yamamoto, K., *Bull. Jpn. Petrol. Inst.* **4,** 15 (1962).
17. Huszár, K., Rácz, G., and Székely, G., *Acta Chim. Acad. Sci. Hungar.* **70,** 287 (1971).
18. Gavalas, G. R., Phichitkul, C., and Voecks, G. E., *J. Catal.* **88,** 54 (1984).
19. Ashcroft, A. T., Cheetham, A. K., Foord, J. S., Green, M. L. H., Grey, C. P., Murrell, A. J., and Vernon, P. D. F., *Nature* **344,** 319 (1990).
20. Vernon, P. D. F., Green, M. L. H., Cheetham, A. K., and Ashcroft, A. T., *Catal. Lett.* **6,** 181 (1990).
21. Gadalla, A. M., and Sommer, M. E., *Chem. Eng. Sci.* **44,** 2825 (1989).
22. Phichitkul, C., Doctoral dissertation, California Institute of Technology, 1981.
23. Gordon, S., and McBride, B. J., "Computer Program for Calculation of Complex Chemical Equilibrium Compositions, Rocket Performance, Incident and Reflected Shocks, and Chapman–Jouguet Detonations," NASA Lewis Research Center, 1976.
24. Gavalas, G. R., Phichitkul, C., and Voecks, G. E., *J. Catal.* **88,** 54 (1984).
25. Ng, K. T., and Hercules, D. M., *J. Phys. Chem.* **80,** 2094 (1976).
26. McIntyre, N. S., Rummery, T. E., Cook, M. G., and Owen, D., *J. Electrochem. Soc.* **123,** 1164 (1976).
27. Vedrine, J. C., Hollinger, G., and Minh, O. T., *J. Phys. Chem.* **82,** 1515 (1978).
28. Wu, M., and Hercules, D. M., *J. Phys. Chem.* **83,** 2003 (1979).